# Downwash airflow distribution pattern of hexa-copter unmanned aerial vehicles

Dengeru Yallappa*, Ramasamy Kavitha, Allimuthu Surendrakumar, Kannan Balaji, Balakrishnan Suthakar, Ayyasamy Paramasivam Mohan Kumar, Yathendranaik Ravi, Narayananaik Ashoka, Kumar Kavan

(*Department of Farm Machinery and Power Engineering, Agricultural Engineering College and Research Institute, Tamil Nadu Agricultural University, Coimbatore*)

**Abstract:** In recent times, the use of vertical take-off and landing (VTOL) multi-rotor Unmanned Aerial Vehicle (UAVs) for spraying chemical pesticides against weeds and pests has recently become popular. The current aerial spray application research is primarily focused on examining the influence of UAV spraying parameters such as flight height, travel speed, rotor configuration, droplet size, payload and wind velocity. The downwash airflow velocity generated by the UAV rotor propeller has a significant impact on the droplet deposition process. A test rig was developed to measure the downwash airflow pattern generated by the rotor propeller of a UAV. In this investigation, a six-rotor electric autonomous UAV sprayer was used to investigate the parameters and distribution laws of downwash airflow velocity. The downwash airflow velocity was measured using portable anemometers mounted on the test rig at radial positions viz., 0 m, 0.5 m, 1 m, 1.5 m and 2 m, perpendicular to (*X*) and parallel to the UAV's flight direction (*Y*). The experiment was conducted at three levels of hover height, viz., 1 m, 2 m and 3 m (*Z*) and three levels of payload, viz., 0 kg, 5 kg, and 10 kg. The special downwash airflow distribution pattern was analysed using the Python programming language (Version 3.7). Results show that the downwash airflow velocity generated by the radial position of the UAV rotor is evenly distributed on the rotating loop and the standard deviation of the downwash airflow velocity is less than 0.5 m/s. The maximum downwash airflow velocity of 13.8 m/s was observed below the rotor at 10 kg payload capacity, 1 m hover height (*Z*), and 0.5 m in the *X*-direction. The minimum downwash wind field of 0.3 m/s was observed at 0 kg pay load capacity, 1 m height, and 2 m in the *X*-direction. The downwash airflow velocity along each position in the radial direction of the rotor increases initially and then decreases. This downwash airflow distribution results helps in mounting of spray nozzle configuration to drone sprayer which helps to understanding spray liquid distribution and other spray operational parameters. The influence of downwash airflow distribution combined with the spray operational parameters of the UAV sprayer *viz.,* flight height, travel speed, rotor configuration, payload and wind velocity on spray volume distribution was studied. A field experiment was conducted to study the effect of UAV sprayer downwash airflow distribution on spray droplet deposition characteristics in a rice crop compared with manual knapsack sprayer.

**Keywords:** downwash air, payload, rotor propeller, flight height, distribution analysis, flight direction

**DOI:** 10.25165/j.ijabe.20241704.7754

**Citation:** Yallappa D, Kavitha R, Surendrakumar A, Balaji K, Suthakar B, Mohan Kumar A P, et al. Downwash airflow distribution pattern of hexa-copter unmanned aerial vehicles. Int J Agric & Biol Eng, 2024; 17(4): 24–34.

## 1 Introduction

Unmanned Aerial Vehicles (UAV) have now become immensely important in various sectors, including agriculture. The use of UAVs with agrochemical spraying attachment systems for crops such as rice, corn, cotton, and sugarcane can effectively avoid the limitation of special field conditions and crop growth on spraying machinery with large wheels, allowing for more efficient, safe, and non-destructive crop protection[1]. Multi-rotor drones have greatly benefited from advanced features in autonomous spraying systems, including autonomous path planning, break point continue to spray, terrain following radar module (auto altitude adjustment), high-precision obstacle avoidance radar, spray task list, spray solution empty indication, battery level warning, and high-accuracy Real Time Kinematics (RTK) location to significantly increase functional stability, efficiency, accuracy, and ease of use[2]. UAVs have the advantages of great mobility and excellent spraying efficiency over traditional land-spraying machines[3].

The most essential benefit of using a multi-rotor UAVs for chemical spraying is that, due to its unique rotor structure and principle of motion, it generates a powerful downwash airflow during flight operation, changing the crop disturbance and improving liquid penetration. As a result, liquid has quite a good deposition impact on the bottom part of crops[4]. The downwash

**Received date:** 2022-06-24 **Accepted date:** 2023-06-05

**Biographies:** **Kavitha R**, PhD, Professor and Head, research interest: mechanization of vegetable crops, groundnut, maize, Email: kavitha@tnau.ac.in; **Surendrakumar A**, PhD, Professor and Head, research interest: farm machinery, application of robotics and sensors in agriculture, Email: surendrakumar@tnau.ac.in; **Balaji K**, PhD, Professor and Head, research interest: remote sensing, Email: balajikannan73@gmail.com; **Suthakar B**, PhD, Associate Professor, research interest: farm machinery, Email: suthaaa@gmail.com; **Mohan Kumar A P**, PhD, Assistant Professor, research interest: fluid power, applied thermodynamics and farm mechanization, Email: apmohankumar@tnau.ac.in; **Ravi Y**, PhD, Scientist, ICAR NRC on Seed Spices, research interest: mechanization of horticultural crops, Email: ravinaiky@gmail.com; **Ashoka N**, PhD, Assistant Professor (COH, Sirsi, UHSB), research interest: agricultural economics, Email: ashokan.abm@gmail.com; **Kavan K**, PhD Research Scholar, research interest: renewable energy, Email: kavankumarreddy07@gmail.com.

***Corresponding author: Yallappa D**, PhD, Research Scholar, research interest: agricultural UAV, farm machinery and renewable energy. Agricultural Engineering College and Research Institute, Tamil Nadu Agricultural University, Coimbatore 641003, India, Tel: +919-422-6611257, Email: yallappa.raravi@gmail.com.

airflow velocity produced by the rotors can create a strong velocity distribution for plants during spraying, helping spray droplets to atomize much further with enhanced deposition onto the crop surface. As a result, spray droplet velocity has positive effects on spray swath, deposition, and drift, influencing the operation's consequences[5].

Lan et al.[6] developed a test rig setup for DJI T16 UAV downwash airflow collection using a wireless wind speed sensor. Luo et al.[7] developed a platform to investigate one-nozzle distribution, which was affected by downwind. Li et al.[8] set up a wind-speed arrays to explore the distribution of downwash in order to assist pollination, a sort of UAV and then the downwash model was fitted using mathematical models such as the Gaussian distribution system. Wu et al.[9] developed a full bridge strain effect principle-based test rig and flexible structure acquisition system for understanding the real-time measurement of the UAV downwash airflow. To simulate one-way fluid-solid coupling interaction, the fluid flow and static structural modules of ANSYS 16.0 finite element software were utilised. Yang et al.[10] used a weather tracker to test the downwash wind speed of the SLK-5 UAV and the highest velocity of the downwash flow was found to be around 10 m/s in the z-direction.

Guo et al.[11] build a computational fluid dynamics (CFD) model of the downwash airflow of the quad-rotor agricultural UAV in hover and explore how the downwash airflow is distributed in the spatial and temporal dimensions. CFD simulation is a novel developing technology and has been commonly used because of its controllable accuracy[12]. For the SLK-5 six-rotor UAV, Yang et al.[13] investigated the effects of downwash and windward airflow on the motion distribution of the droplet group, using a combination of computational fluid dynamics and radial basis neural networks. Yang Bai et al.[14] investigated the downwash flow velocity distribution of a lab-scale rotor simulator to understand the impact of the blades rotational speed and axial distance on the velocity intensity and it was concluded that, the spatial velocity distribution shows higher values with an increase in rotational speed and axial distance closer to the rotor blade. Yang et al.[10] studied the influence of UAV rotor downwash airflow spray width using the XV-2 model. Dixon et al.[15] investigated the effect of flying height on droplet deposition. They state that when the flying height increases, the vertical velocity of the UAV downwash flow near the crop canopy will decrease. Wang et al.[16] investigated the downwash of a single-rotor UAV, 3WQF80-10, using water-sensitive paper to enhance the spatial quality balance of droplets, and then assessed the downwash distribution of three different types of UAVs based on droplet deposition in different layers. Tang et al.[17] conducted the droplet distribution influenced by eight rotors using Particle Image Velocimetry (PIV) technology and it was observed that the downwash velocity not only changes the deposition zone of the droplets, but also influenced their distribution. Lan et al.[6] conducted research on the impact of the UAV downwash on droplet deposition distribution using a DJI T16 UAV, and it was found that with an increase in flight height, the change of the downwash wind field led to a gradual decrease in droplet deposition in the effective spray area and were deposited more uniformly[18]. The above studies indicate that the relationship between UAV spray operational parameters and downwash airflow distribution have been explored and the influence of downwash airflow on droplet penetration and spray volume distribution has also been studied.

Normally electronic devices, such as wireless anemometers, wind-speed arrays, PIVs, cameras, and CFD simulation are used for downwash measurement. There are no sensors specifically developed for detecting downwash flow and distribution on large scales. There are few research on multi-rotor UAVs' downwash measurement technique. As a result, a unique downwash airflow collection test rig was developed to measure and analyse the velocity distribution at various points within the downwash airflow pattern generated during rotor rotation. Wang et al.[19] investigated the simulation and examined the impact of the inner tilt angle on the downwash airflow field using the Reynolds average NS equation and RNG k- turbulence model.

Using the XV-2 model, Yang et al.[20] investigated the impact of VTOL drone sprayer downwash airflow pattern on spray width. The findings indicated that the drone sprayer height of spray mostly affected the spray width, with a 6 m spray height producing an effective spray width of 10 m. According to Zhang et al.[21] numerical analysis of the quad-rotor unmanned aerial vehicle's downwash flow field; the downwash flow field is significantly influenced by the drone's flying velocity. When the flying speed hits 6 m/s, the wingtip vortex velocity reaches 3.3 m/s, which significantly raises the probability of droplet drift and has a severe entrainment effect on the droplets. Berner and Chojnacki[22] tested the correlation between the VTOL drone multi rotors rotational speed and spray deposition. Choi et al.[23] tested a six-rotor UAV with three operational spray heights and two operational forward travel speeds. Zhang et al.[24] conducted Downwash airflow field distribution characteristics using DJI T30 six-rotor plant protection UAV and recommended that the flight height during field spraying operations should not exceed 3.2 m.

Wang et al.[25] investigated the vertical downwash airflow of a one rotor drone sprayer (3WQF80-10), using water-sensitive paper to enhance the spray droplets, and then assessed the downwash airflow distribution of three different types of UAVs based on droplet deposition in different layers. Liu et al.[26] studied the wind velocity distribution of the rotor downwash flow field at various elevations using the LTH-100 single-rotor agricultural UAV. According to the simulation results for the hover state, the peak velocity in the flow field is distributed in a circular pattern just below the rotor's distal axis. Tang et al.[27] conducted the droplet distribution influenced by eight rotors using Particle Image Velocimetry (PIV) technology and it was observed that the downwash airflow distribution velocity not only changes the spray droplet deposition zone, but also influenced their spray droplet distribution pattern.

## 2 Materials and methods

Test rig was developed at Agricultural Machinery Research Centre (AMRC), Department of Farm Machinery and Power Engineering, Agricultural Engineering College and Research Institute, Tamil Nadu Agricultural University, Tamil Nadu, India to understand the mechanism of the downwash airflow distribution system produced by the rotors of the UAV. The ultimate purpose of downwash research is to understand the airflow pattern distribution system and clarify the downwash airflow distribution system.

### 2.1 Equipment

The UAV used in the present investigation was an E610P six-rotor electric UAV sprayer (EFT Electronic Technology Co., Ltd., Hefei City, China), as shown in Figure 1. The six rotor UAV sprayer mainly consists of BLDC motors, lithium polymer (LiPo) batteries, flight controller, RC receiver, GNSS RTK unit, chemical tank, spray pump, nozzles, and supporting frame. The UAV has two LiPo batteries of 6 cells each with a capacity of 16 000 mA·h to

supply the necessary current required for the propulsion system and a 10 L loading capacity chemical tank. A 12 V BLDC motor is coupled with a pump to pressurise spray liquid and then to atomize it into fine spray droplets. This UAV sprayer has four numbers of 2020A-132 series flat fan nozzles (Ningbo Licheng Agricultural Spray Technology Co., Ltd., Zhejiang, China), which are mounted and screwed below the BLDC motor base plate. The UAV has the functions of GPS route planning and breakpoint return, which can complete aerial spraying operations autonomously. The specifications of UAV agricultural spraying are listed in Table 1.


1. Flight Controller and Sensors 2. BLDC motor arm 3. Fluid hose pipe 4. BLDC Motor 5. Flat fan nozzle 6. Pesticide tank 7. Landing gear 8. Foldable propeller 9. LiPo Battery

Figure 1 Six rotor battery operated autonomous UAV sprayer

**Table 1 Specification of UAV agricultural sprayer**

| Main parameter | Norms and value |
|---|---|
| Type | Hexacopter |
| Item model | E610P |
| Unfold fuselage size (L×W×H)/mm | 2000×1800×670 |
| Folding size (L×W×H)/mm | 950×850×670 |
| Power source | 12S 16,0000 mA·h LiPo Battery |
| Payload capacity/L | 10 |
| Self-weight/kg | 6.9 |
| Take-off weight/kg | 26 |
| Flight height/m | 1-20 |
| Forward travel speed/m·s$^{-1}$ | 0-8 |
| Type of spray nozzle | Flat fan shape (2020A-132 series) |
| Number of nozzles | 4 |
| Discharge rate/L·min$^{-1}$ | 0-3.2 |
| Swath width of spray/m | 3-5 |
| Liquid pressure/kg·cm$^{-2}$ | 3.4 |
| Remote controller distance, km | 1.5 |
| No-load flight time/min | 25 |
| Charging time/min | 90 |

2.1.1 Rotors (six rotor) working configuration of UAV sprayer

Figure 2 depicts the six-rotor UAV's movement laws. The six rotors are evenly spaced around the circumference, the rotor support arms are of equal length, the included angle between any two arms is 60°, and the rotation directions of subsequent rotors are opposite.

The absolute ground coordinate systems are $O_e$, $X_e$, $Y_e$, and $Z_e$ in Figure 2, whereas the relative coordinate systems of the six-rotor UAV system are $O_b$, $X_b$, $Y_b$, and $Z_b$. Each motor's lifting forces ($f_i$, $i$ = 1, 2, 3, 4, 5, 6) are proportional to the square of the rotor's rotational speed, and the UAV's flight attitude (composed of the, $\Psi$, $\theta$, and $\Phi$ corners) can be adjusted to meet payload by modifying the speed of the six motors. When the rotational speed of each rotor is increased, the total lifting force is sufficient to overcome the gravity of the UAV itself, and the UAV lifts. The UAV sprayer, on the other hand, declines by decreasing the rotating speed of each rotor until the total lifting force is less than gravity. Similarly, when the lift produced by the rotors and the gravity of the UAV sprayer are equal, the UAV sprayer will hover condition. The technical parameters of the multi-rotor motor and propeller are listed in Table 2.

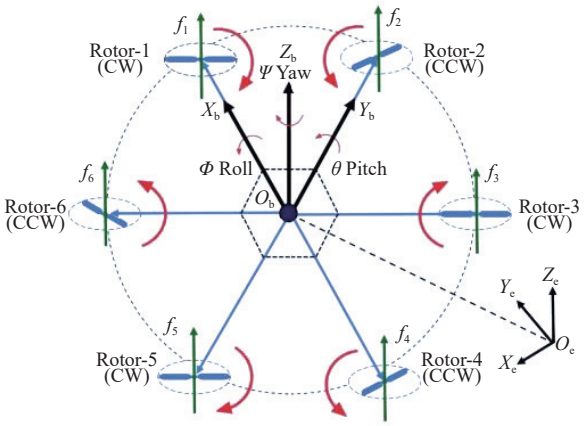


Figure 2 Motion system of the six rotor UAV sprayer

**Table 2 Technical parameters of multi-rotor and propeller of UAV**

| | Main parameter | Norms and value |
|---|---|---|
| Motor | Brand | HOBBYWING |
| | Number of rotors, unit | 6 |
| | Motor model | 6215 (180 K RTF) |
| | Rotor outer diameter, mm | 70 |
| | KV rating | 180 |
| | Operating temperature/°C | –20 to 50 |
| | Max. thrust/kg | 11.9 |
| | Recommended load/motor/kg | 3-5 |
| Propeller | Size/mm | 584 |
| | Type | Foldable |
| | Size | 2388 V2 Inch |

2.1.2 Wind flow distribution system of hex copter UAV sprayer

Figure 3 shows the motors rotation law of the UAV hexa-copter model. The adjacent wing, rotor 1, rotor 3, and rotor 5 rotate in a clockwise direction. Rotor 2, rotor 4, and rotor 6 all rotate counter-clockwise. The rotation directions of rotor 1 and rotor 2 are opposite, while both rotors induce flow into the inner circle. On the contrary, the rotor 2 and rotor 3 induce flow to the outer circle. The airflow induced and outflow are indicated as green arrows and red arrows, respectively.

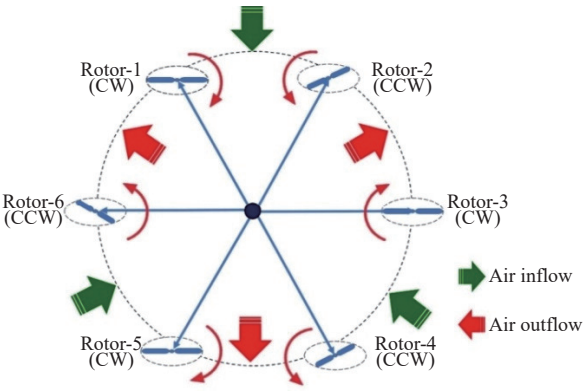


Figure 3 Wind flow distribution in two motion states of adjacent wings

**2.2 Development of downwash airflow measurement test rig**

A special test rig was developed at Agricultural Machinery Research Centre (AMRC), Department of Farm Machinery and

Power Engineering, Agricultural Engineering College and Research Institute, Tamil Nadu Agricultural University, Coimbatore, Tamil Nadu, India to study and understand the mechanism of the downwash airflow distribution pattern produced by the propeller of a six-rotor UAV sprayer at different hover heights and different payload capacities.

The frame of the downwash airflow measurement test rig was developed according to the position of rotors in six-rotor UAV, with a horizontal distance between two rotors of 1.42 m. In addition, the diameter of the propeller is 20 cm. The developed test rig consisted of four numbers of mild steel (M.S) rectangular hollow pipes of size 50 mm×25 mm×2 mm as a base structure and supported vertically with four numbers of equal M.S angle iron of 40 mm×40 mm×3 mm. Another four numbers of M.S. rectangular hollow pipe (50 mm×25 mm×2 mm) were placed on top of the support frame, which accommodates the Light Detection and Ranging (LIDAR) distance metre instrument (DEKOPRO, LRE520 80M) and airflow measuring anemometer points at the desired positions. A 2.5 m length of hollow M.S. square pipe (20 mm×20 mm×2 mm) welded with M.S. flat iron of size 25 mm×2 mm clamp for holding the anemometer impeller and display was provided. Five anemometers (LUTRON AM 4202, Vane type, rang: 0.4-30.0 m/s) were placed horizontally on a 2.5 m long M.S square pipe (20 mm×20 mm×2 mm) at intervals of 0 m, 0.5 m, 1.0 m, 1.5 m and 2.0 m perpendicular to the flight direction of the UAV (*Y*). One end of M.S. square pipe was mounted at central part of the test rig frame with nut and bolt and another end was supported vertically with an M.S. square pipe (20 mm×20 mm×2 mm) stand with a base wheel for easy rotation in 360°. The developed test rig for measuring multi rotor UAV downwash airflow is shown in Figure 4.


a. Anemometer b. Portable laser radar on board the frame c. Complete view of test rig d. Top view of test rig

Figure 4 The developed test rig for measuring multi rotor UAV downwash airflow

### 2.3 Arrangement of downwash airflow collection sampling points

The purpose of this test is to investigate the distribution system of UAV downwash airflow velocity of rotors in the horizontal cross-section with different payload capacities and different hover heights. The layout of the downwash airflow velocity measurement points is as shown in Figure 5.

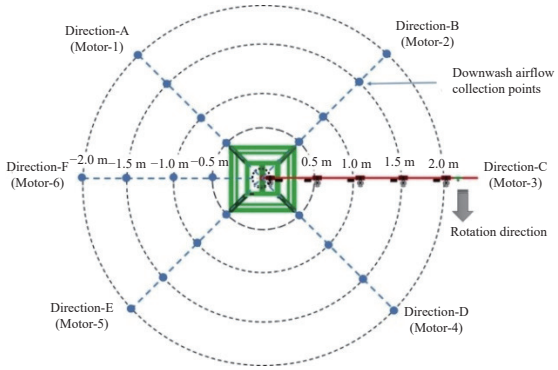


Figure 5 Schematic layout of location of downwash airflow pattern collection points

To measure the downwash airflow velocity at different radial positions of rotor propellers, five measurement points are set at an interval of 0.5 m from the radial centre point. The selected UAV model has hex copters, six measuring point directions (*A*, *B*, *C*, *D*, *E*, and *F*) were respectively arranged at intervals of 60° on each equal-diameter ring. The UAV downwash airflow velocity was recorded in all six directions of rotors for three hover heights and three payload capacities. Five anemometer readings were recorded in direction-*A* (rotor-1) and in direction-*B* (rotor-2) anemometer readings were recorded by clockwise rotation of the mounted anemometer support stand. Simultaneously downwash airflow readings for *C*, *D*, *E*, and *F* directions were recorded. Figure 6 indicates the downwash airflow distribution collection points in a radial direction.

### 2.4 Test and collection sampling points of downwash airflow distribution pattern at outdoor condition

The multi rotor UAV downwash airflow pattern test was conducted at Agricultural Machinery Research Centre (AMRC), Department of Farm Machinery and Power Engineering, Agricultural Engineering College and Research Institute, Tamil Nadu Agricultural University, Tamil Nadu, India. To record and understand the mechanism of the downwash airflow pattern, the UAV was hovered at different flight heights viz., 1.0 m, 2.0 m, and 3.0 m (*Z*) and three levels of payload viz., 0 kg, 5 kg and 10 kg. These are independent variables that mainly influence the functional performance of the UAV downwash airflow distribution pattern system. A laser distance metre instrument was mounted on the above test rig to measure the hover height (the distance between the tips of the rotor propeller to the anemometer impeller). The details of the parameters with variables are presented in Table 3. The downwash airflow velocity was recorded in *X*- and *Y*-directions using a digital anemometer (LUTRON AM 4202, Vane type, rang: 0.4-30.0 m/s) for each of the UAV rotor directions (*A*, *B*, *C*, *D*, *E* and *F*) by rotating the anemometer mounted pipe in a clockwise direction. This test experiment was conducted at three hover heights and three levels of payload and downwash airflow velocity was measured at 0 m, 0.5 m, 1.0 mm, 1.5 m and 2.0 mm lateral distance from the centre point. Each treatment was replicated three times. The schematic diagram of UAV downwash airflow pattern test at outdoor condition is shown in Figure 6. The downwash distribution airflow collection points were arranged and recorded at 30 measuring points in the plane coordinate system for three hover heights and three payload capacities. The downwash airflow distribution pattern was analysed. Experimental setup of multi rotor UAV downwash airflow pattern test at outdoor condition is shown in Figure 7. This downwash airflow velocity test site and procedure were followed as per Lan et al.[6] , Yang et al.[13] and Tan et al.[28]

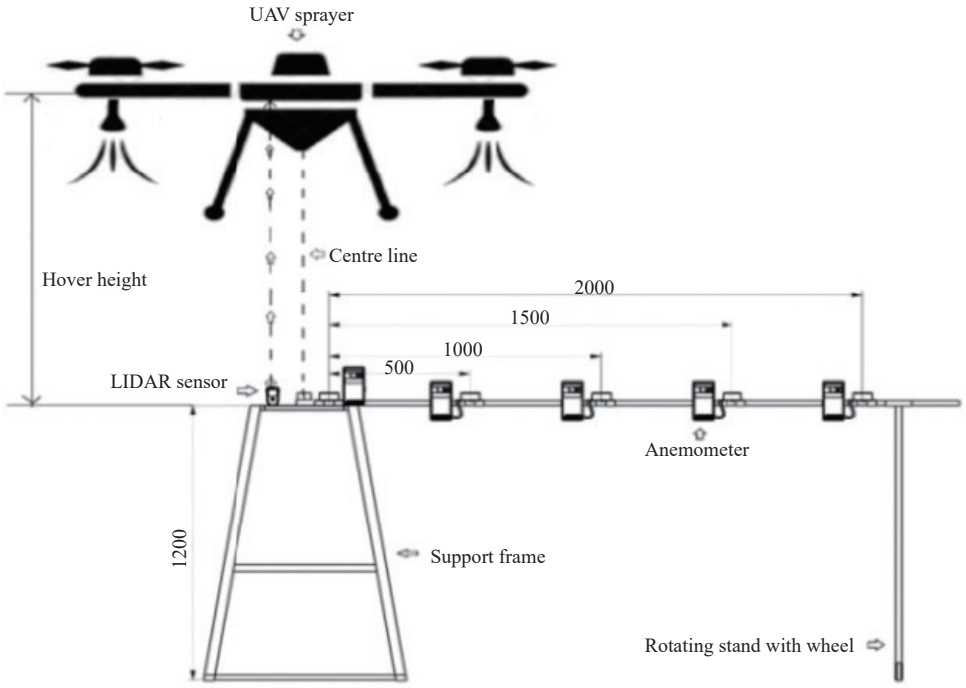


Figure 6 Schematic diagram of UAV downwash airflow pattern test at outdoor condition

**Table 3 Variables with selected levels for analysing the UAV downwash airflow pattern**

| Variables | Parameters | Symbol | Levels |
|---|---|---|---|
| Independent | Payload/kg | $P_1$, $P_2$, $P_3$ | 0, 5, 10 |
| | Height of hover/m | $H_1$, $H_2$, $H_3$ | 1.0, 2.0, 3.0 |
| | Location of anemometer/m | $L_1$, $L_2$, $L_3$, $L_4$, $L_5$ | 0, 0.5, 1.0, 1.5, 2.0 |
| Dependent | Downwash airflow velocity/m·s$^{-1}$ | | |

Figure 7 Experimental setup of multi rotor UAV downwash airflow pattern test at outdoor condition

### 2.5 Standard deviation analysis of downwash airflow distribution velocity

The standard deviation of the data reflects the degree of dispersion of a set of data and the average value[15]. The deviation is calculated according to the following equation:

$$\sigma = \sqrt{\frac{\sum_{1}^{N}(X_i - X)^2}{N-1}}$$

where, $\sigma$ is standard deviation, m/s; $N$ is the number of samples; $X_i$ is the sample value, m/s; $X$ is sample mean.

The standard deviations of six measurements of downwash airflow velocity were calculated for each radial position at each measurement height level. The effects of payload and hover height on downwash airflow distribution pattern of UAV were assessed and data were analysed using Python programming language (Version 3.7).

### 2.6 Recording of meteorological parameters during UAV downwash airflow distribution test

During the UAV downwash airflow pattern test, the different meteorological parameters such as wind velocity, air temperature, humidity, and rainfall were recorded. A portable anemometer was mounted on a square iron pipe (20 mm×20 mm×2 mm) at 2 m above the ground level to measure the wind velocity[29]. Weather conditions, including wind speed, air temperature, and relative humidity during the study, are listed in Table 4.

**Table 4 Meteorological data during the UAV downwash airflow pattern test**

| | |
|---|---|
| Date | 04.01.2022, 06.01.2022 and 07.01.2022 |
| Time | 08:30 AM, 5:30 PM and 6:00 PM |
| Location | Agricultural Machinery Research Centre, Dept. of Farm Machinery and Power Engineering, AEC&RI, TNAU, Coimbatore, Tamil Nadu, India (11.012 774°N, 76.927 036°E) |
| Environmental parameters | Air temperature: 28.3°C -30.9°C<br>Relative humidity: 54.5%-60.2%<br>Wind velocity: 0.11 to 0.21 m·s$^{-1}$<br>Rainfall: 0 mm |

### 2.7 Field test

Influence the drone sprayer downwash airflow distribution of UAV sprayer on spray droplet deposition characteristics experiment was carried out at the Wetland field (11.003 247°N, 76.924 474°E), Tamil Nadu Agricultural University, Coimbatore, Tamil Nadu state, India. A battery-operated knapsack sprayer (m/s, Kisan Kraft, KK-BBS199, 16 L capacity) was used to spray the solution as a control treatment. The layout of the rice crop research plot and arrangement and locations of WSP samples on rice crop leaf for UAV spray and manual spray are shown in Figure 8. The details of crop parameters were measured during the spraying operation and are listed in Table 5.

#### 2.7.1 Arrangement of spray droplet deposition samples

During the experiment, a type of spray card called water-sensitive paper (made by AAMS, Maldegem, Belgium). Its surface is dye-coated, and aqueous droplets that land on it leave visible

stains[30]. The number of spray droplets deposited on the surface of the leaves at three different locations was measured using a water sensitive paper samples[31,32]. As illustrated in Figures 9 and 10, the water-sensitive paper (WSP) was clamped with a double-ended clip at each sampling location and retained on the leaves at two distinct plant heights, namely 0.45 m and 0.75 m above the ground.

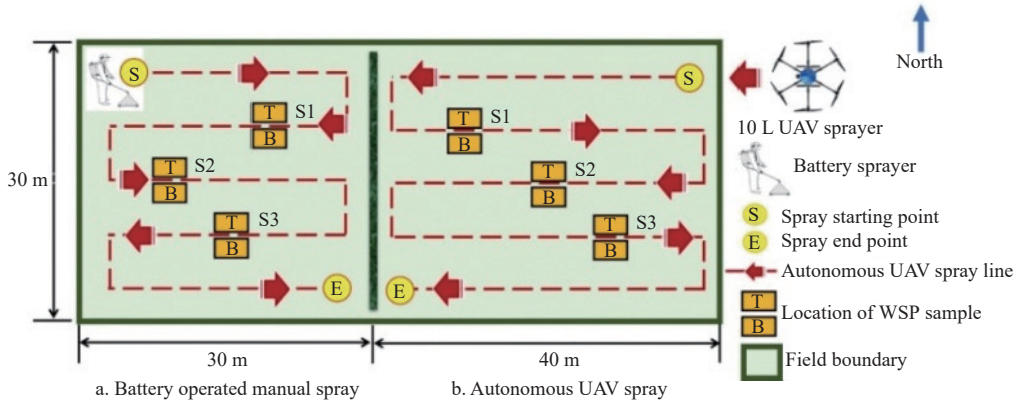


Figure 8 Layout of rice crop field and placement of WSP spray samples

**Table 5 Specific crop parameters**

| Crop parameters Norms and numerical value | |
|---|---|
| Crop | Rice |
| Variety | Co51 |
| Date of plantation | 08.01.2022 |
| Height of crop/mm | 750-830 |
| Stage of crop | Flowering stage (68 d) |
| Number of tillers per plant | 37 |
| Number of panicles/m$^{-2}$ | 320 |

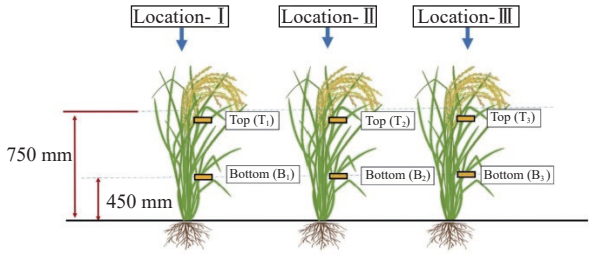


Figure 9 Layout of WSP samples in upper ($T_1$, $T_2$, $T_3$) and bottom ($B_1$, $B_2$, $B_3$) on rice crop leaf in field

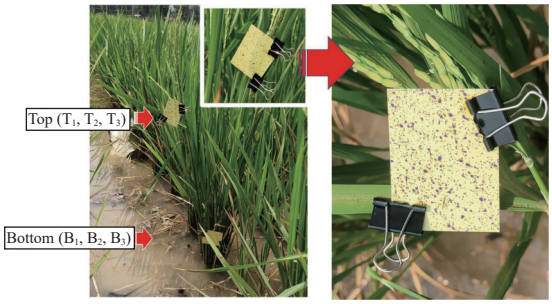


Figure 10 Position of WSP samples on rice crop leaf in field

2.7.2 Recording of meteorological parameters during spray droplet deposition

Several meteorological parameters, including natural wind speed, air temperature, humidity, and rainfall, have an impact on the effectiveness of UAV and manual spraying operations. To measure the natural wind speed, a portable anemometer (LUTRON, model: AM 4202, type: Vane, range: 0.4-30.0 m/s) was fixed on a square iron pipe at a height of 2.0 m above the crop canopy[29]. Table 6 lists the various meteorological parameters were noted during the investigation.

**Table 6 Meteorological reports while conducting UAV and manual spray in a rice agricultural field**

| | | |
|---|---|---|
| Location | Wetland field (N11.003247, E76.924474), TNAU, Coimbatore, Tamil Nadu state, India | |
| Environmental parameters | Air temperature/°C | 25.8 to 31.4 |
| | Relative humidity/% | 55.7 to 60.3 |
| | Natural wind velocity/m·s$^{-1}$ | 1.1 to 1.5 |
| | Rainfall/mm | 0 |

2.7.3 Water sensitive paper (WSP) sample acquisition and spraying effectiveness analysis

After every spraying test, WSPs were immediately collected and transferred to the laboratory for further study. The uniformity of spray deposition is expressed as VMD (Volume median diameter), NMD (Numeric median diameter) and Uniformity coefficient (VMD/NMD ratio). According to the method of Zhu et al.[33] the deposit amount and coverage density of the droplets at upper and bottom locations were analysed.

## 3 Results and discussion

To investigate the distribution pattern of downwash airflow velocity in horizontal and vertical sections under the UAV six rotors, the central position of the UAV model is utilised as the origin of coordinates to establish the plane coordinate system of downwash airflow distribution at each height plane[9,13,28]. The downwash distribution airflow collection points were arranged and recorded at 30 measuring points in the plane coordinate system. The standard deviations of six measurements of downwash airflow velocity data for each radial position viz., 0 m, 0.5 m, 1.0 m, 1.5 m and 2.0 m at each hover height level viz., 1.0 m, 2.0 m and 2.0 m, the results are presented in Figure 11.

The histogram in Figure 12 indicates the standard deviation of average downwash airflow velocity measurements in six motor directions (*A*, *B*, *C*, *D*, *E*, and *F*) at five positions (0 m, 0.5 m, 1.0 m, 1.5 m to 2.0 m) rotating in three different hover height (1.0 m, 2.0 m and 3.0 m). There are some variances in the standard deviation of downwash velocity at different airflow collation points in the same hover height and payload. The standard deviation gradually increases and then decreases as the hover height and payload increased, implying that the distribution of the downwash airflow velocity values at each measurement point increases and similar result trend was found by Yang et al.[10] and Tan et al.[28] The overall standard deviation, however, is less than 0.5 m/s.

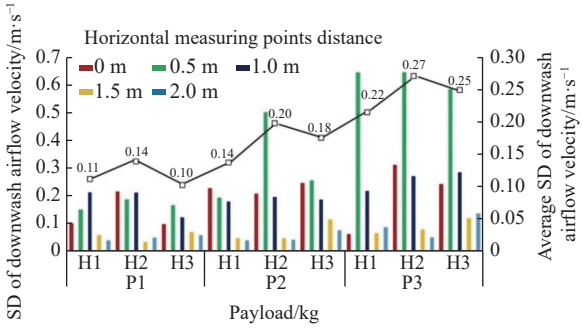


Figure 11 Standard deviation of downwash airflow velocity at different hover height and payload

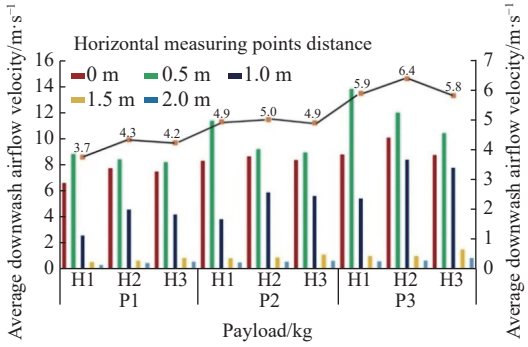


Figure 12 Average downwash airflow velocity at different hover height and payload

Figure 12 indicates that the average downwash airflow velocity produced from the UAV central part to the rotor propeller wingtip position changes, increasing first and then decreasing. At 10 kg payload capacity, 1.0 m height, and 0.5 m distance in the *X*-direction, the greatest average downwash airflow velocity of 13.8 m/s was observed. At a 0 kg payload capacity, 1.0 m height, and 2.0 m distance in the *X*-direction, a minimum downwash airflow velocity of 0.3 m/s was measured. The downwash airflow velocity generated at the UAV rotor propeller end does have smallest value.

The average downwash airflow velocity at the central point (0 m) of UAV shows a trend of increasing initially and then decreasing with increasing UAV hover height. This suggests that the outer downwash airflow compresses the inner rotor section's downwash velocity, resulting in an increase in both airflow density and downwash airflow velocity. The density decreases as a result of the diverging lateral airflow, resulting in a decrease in downwash airflow velocity and similar results were found by Tan et al.[28] The average downwash velocity values at the 0.5 m and 1.0 m distance positions decrease gradually as hover height increases, indicating that the downwash airflow velocity generated in the middle of the UAV rotor first compresses inwards before diverging outwards, resulting in a decrease in vertical airflow density at the position and a decrease in downwash velocity. With increasing hover height, the downwash velocity produced at the 1.5 m and 2.0 m positions reduces. Finally, the overall trend of the downwash airflow velocity below the UAV rotor is the parallel in the middle and then diffusion at the end and same results were found by Wu et al.[9] and Tan et al.[28]

### 3.1 Effect of payload on downwash airflow distribution in heights of hovering

According to the layout scheme, the downwash airflow velocity distribution cloud diagram at each hover height level and payload were plotted by interpolation with the use of the Python software. Figures 13-15 present the average downwash airflow velocity at all the measurement points under 0 kg, 5.0 kg and 10.0 kg payload and 1.0 m, 2.0 m and 3.0 m hover height.

Figures 13-15 show the downwash airflow velocity at different heights (*Z*-direction) on the 'YOZ' section and the *XOZ* section after analysing the spatial downwash airflow distribution system. The peak value of downwash airflow velocity in the centre reached 6.73 m/s, and the airflow directly below the UAV model centre was significantly lower than that on both sides. This may be mainly due to the low hover height of the UAV, resulting in insufficient space for the downwash airflow velocity on both sides of the rotor to spread out fully. The maximum downwash wind field of 13.8 m/s was observed at 10 kg payload capacity, 1.0 m height, and 0.5 m in the *X*-direction. The minimum downwash wind field of 0.3 m/s was observed at 0 kg pay load capacity, 1.0 m height, and 2.0 m in the *X*-direction. Two "valleys" are indicated in the centre. As the downwash airflow velocity continues to flow downward and meet, the two "peaks" on the outside decrease and disappear. As the vertical distances from the rotor increase, the edges of the downwash airflow merge more and more, and the "peak" difference minimizes and similar results were fund by Yang et al.[13] With the increase in altitude, the boundary of downwash velocity generated at each location is gradually reduced, and the distribution of downwash velocity at the section becomes more uniform. Similar trend was observed by Yang et al.[13] The downwash airflow velocity generated at a 0.5 m radial distance from the centre has the largest downwash velocity below the rotor. At the near-ground end (2.0 m), the downwash velocity weakens due to the influence of the airflow field ground effect.

### 3.2 UAV spray droplet deposition rate and distribution characteristics analysis

The WSPs samples were mounted with pin on the rice crop leaf at 0.2 m and 0.4 m from the ground surface level. Upper and lower layers were distinguished between the sampling sites. The actual spray droplet deposition level of the sprayed droplets is represented by the important indicator referred to as droplet deposition. Each WSP samples of spray droplet size, droplet density, droplet deposition, droplet area coverage, droplet deposition rate, and uniformity of deposition were determined and analysed using Deposit Scan software and the results are listed in Table 7.

The UAV sprayer was operated at a forward speed of 3.5 m/s at a spray height of 1.3 m (the crop canopy) with the natural wind speed of 1.8 m/s. The spray droplet characteristics, viz., spray deposition rate ($\mu$L/cm$^2$), spray droplet size ($\mu$m), spray deposition density (droplets/cm$^2$) and spray deposition uniformity (%) were analysed using instruments of stereo micro and macro scope and then all scanned images were processed with DepositScan software. The average spray droplet deposition rate in the upper layer and bottom layer was found to be 0.89 $\mu$L/cm$^2$ and 0.80 $\mu$L/cm$^2$ respectively, for UAV sprayer and 1.31 $\mu$L/cm$^2$ and 0.29 $\mu$L/cm$^2$ respectively, for manual sprayer (KK-BBS199). The average spray coverage per unit area in the upper layer and bottom layer was found to be 8.83% and 8.36%, respectively, for the UAV sprayer and 10.30% and 2.86%, respectively, for the knapsack sprayer. This is due to the downwash airflow produced the rotors propeller of drone sprayer has positive significance on the rice crop canopy and helps in uniform droplet distribution in the upper and bottom layers[30]. Similar results were obtained by Xue[1] using UAV sprayer in paddy field. The average spray droplet deposition densities on the upper layer and lower layers are 36.66 and 30.66 droplets/cm$^2$ respectively, for the UAV sprayer and 41.0 and 13.0 droplets/cm$^2$,

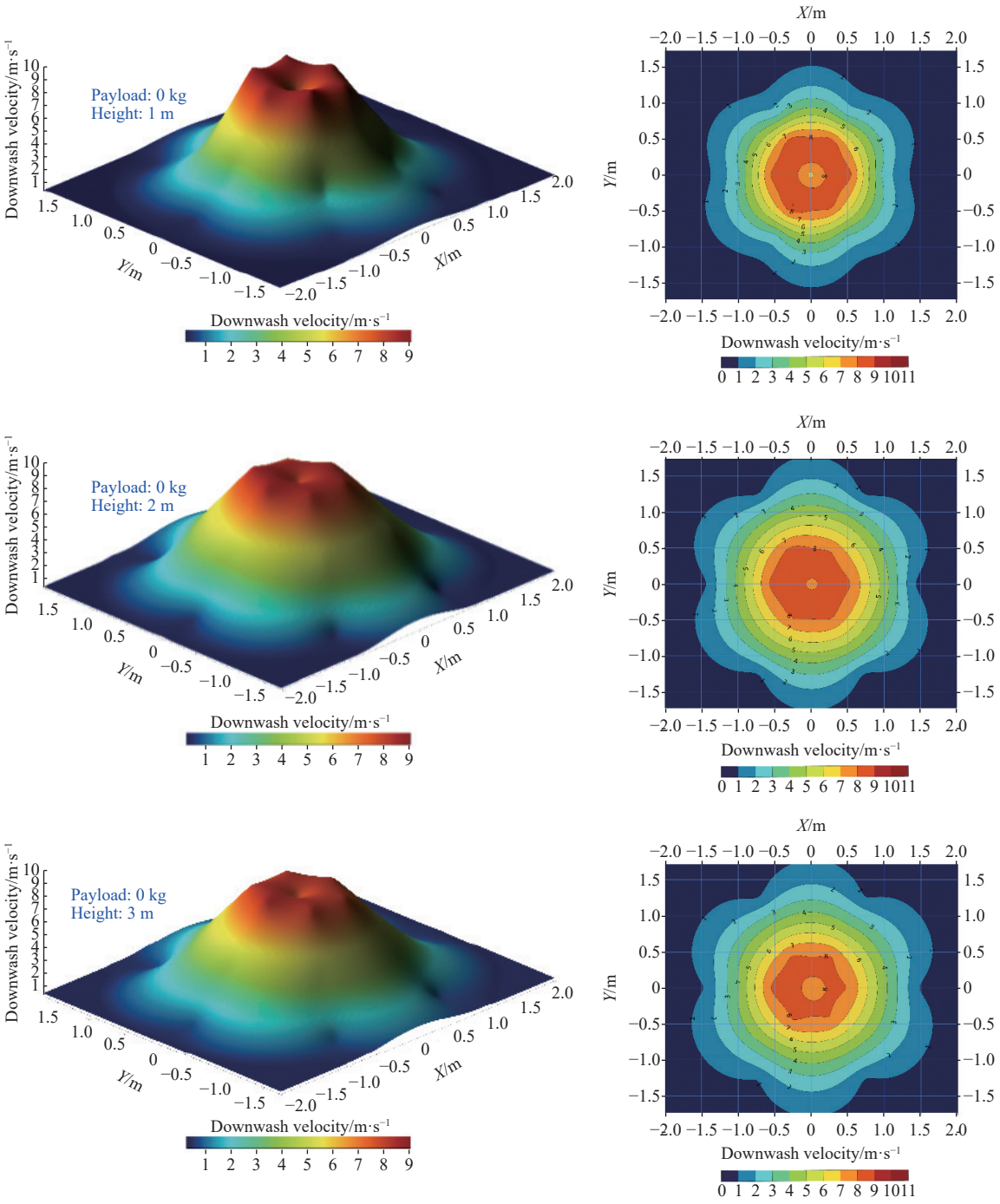


Figure 13 Downwash airflow distribution velocity at 0 kg payload (1000, 2000 and 3000 mm)

respectively, for the knapsack sprayer. The spray deposition uniformity was better in the upper layer and bottom layer with the relatively smaller values of CV value 4.2% and 8.2% respectively using UAV sprayer compared to knapsack sprayer with uneven deposition uniformity in upper (8.0%) and bottom layer (14.8%), respectively. UAV spraying technology showed better results in spray droplet deposition rate, spray coverage per unit area and more well spray droplet deposition densities than the conventional battery-operated manual sprayer. The downwash airflow also contributes to improving the spray droplet distribution in the downwash area because of the higher speed rotation of the rotor propeller of UAV sprayer[20,34,35].

## 4 Conclusions

A multi-rotor battery-operated UAV sprayer (10 L) was used to investigate the downwash airflow velocity distribution pattern generated by rotor propellers. A special test rig was developed for collecting the downwash airflow velocity distribution of the propeller rotor. The downwash airflow velocity distribution below the rotor was measured at three hover heights viz., 1.0 m, 2.0 m and 3.0 m and three payloads viz., 0 kg, 5 kg and 10 kg. The results were analysed and following conclusions were obtained:

1) The downwash airflow velocity generated by each position is different from the centre of the UAV to the rotor wing. With the increase in radial distance from 0.5 m the downwash velocity increases first and decreases later.

2) The maximum downwash airflow velocity of 13.8 m/s was observed below the rotor at 10 kg payload capacity, 1.0 m hover height (*Z*-direction), and 0.5 m in the *X*-direction. The minimum downwash airflow velocity of 0.3 m/s was observed at 0 kg pay

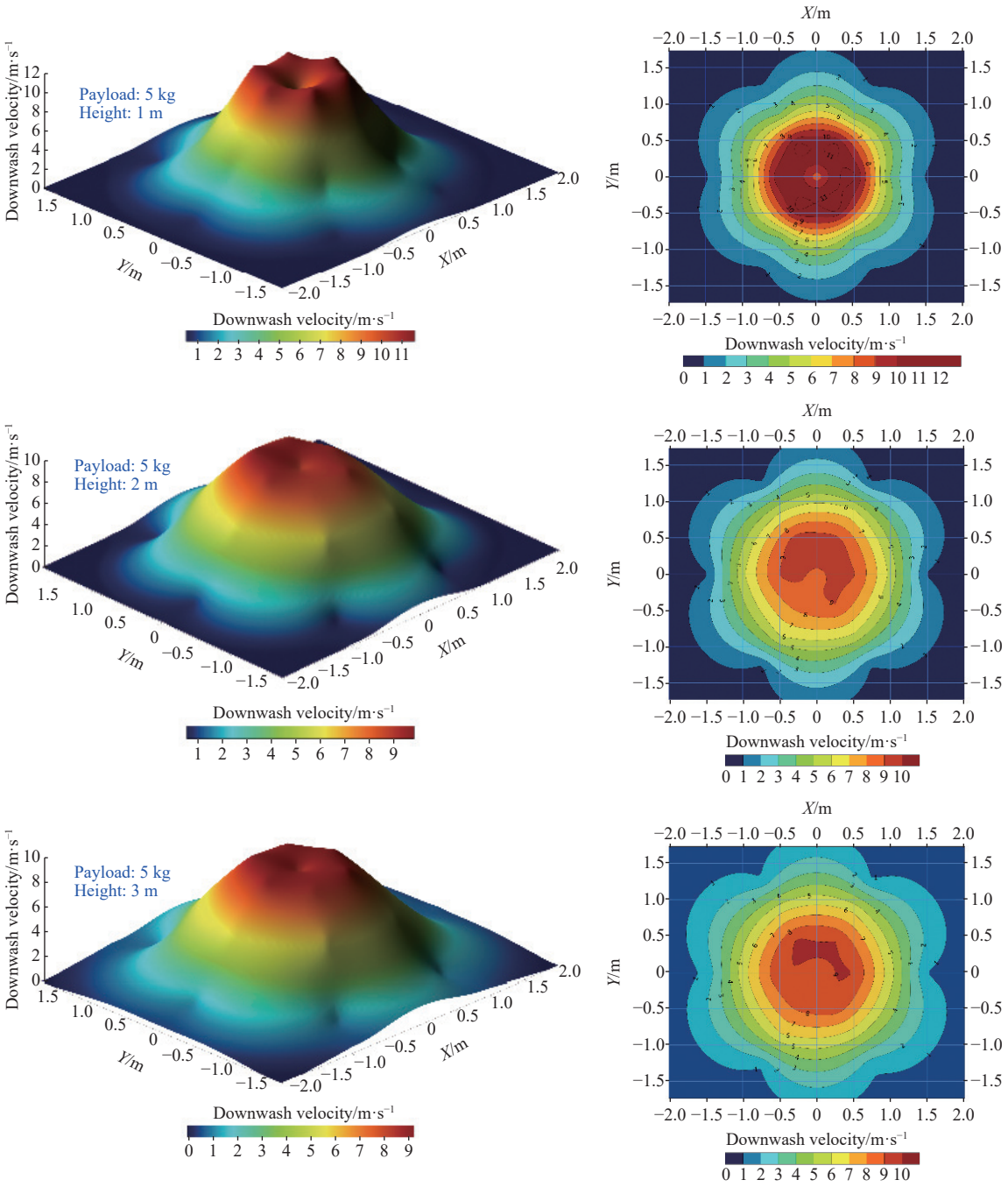


Figure 14 Downwash airflow distribution velocity at 5 kg payload (1000, 2000 and 3000 mm)

load capacity, 1.0 m height, and 2.0 m in the *X*-direction.

3) The results showed that there were obvious differences in the distribution of the downwash flow pattern of the UAV at three hover heights and three payloads. As the hover height increased below the rotor, the downwash airflow velocity in the *X*-direction and *Z*-direction showed a strong to weak trend, while the downwash airflow velocity in the *Y*-direction showed the opposite trend. The airflow velocity gradually spreads to the surroundings, and the area covered by the downwash gradually increases.

4) As the downwash airflow velocity continues to flow downward and meet, the two "peaks" on the outside decrease and disappear. As the vertical distances from the rotor increase, the edges of the downwash airflow merge more and more, and the "peak" difference minimizes.

5) There was almost equal deposition rate in upper layer (0.89 $\mu$L/cm$^2$) and bottom layer (0.80 $\mu$L/cm$^2$) using UAV sprayer compared to manual knapsack sprayer in upper (1.31 $\mu$L/cm$^2$) and bottom layer (0.29 $\mu$L/cm$^2$) respectively.

6) Overall, spray droplet reaches the bottom of the crop leaf due to the effect of UAV downwash airflow whereas spray droplet does not reach in the bottom layer with knapsack sprayer.

7) The UAV spray method helps in even coverage per unit area in the upper and bottom layers of 8.83% and 8.36% respectively compared to manual spray method in upper and bottom layer as 10.5% and 2.2%, respectively. Hence the UAV multi-rotor downwash airflow had a positive impact on the spray droplet deposit rate in the rice crop.

8) The results of this study provide references for the arrangement of nozzles in the airflow pattern below the rotor and establishes a reference for the spatial motion trend analysis of the spray volume distribution in the rotor-downwash airflow.

9) Result helps in establishing the downwash airflow

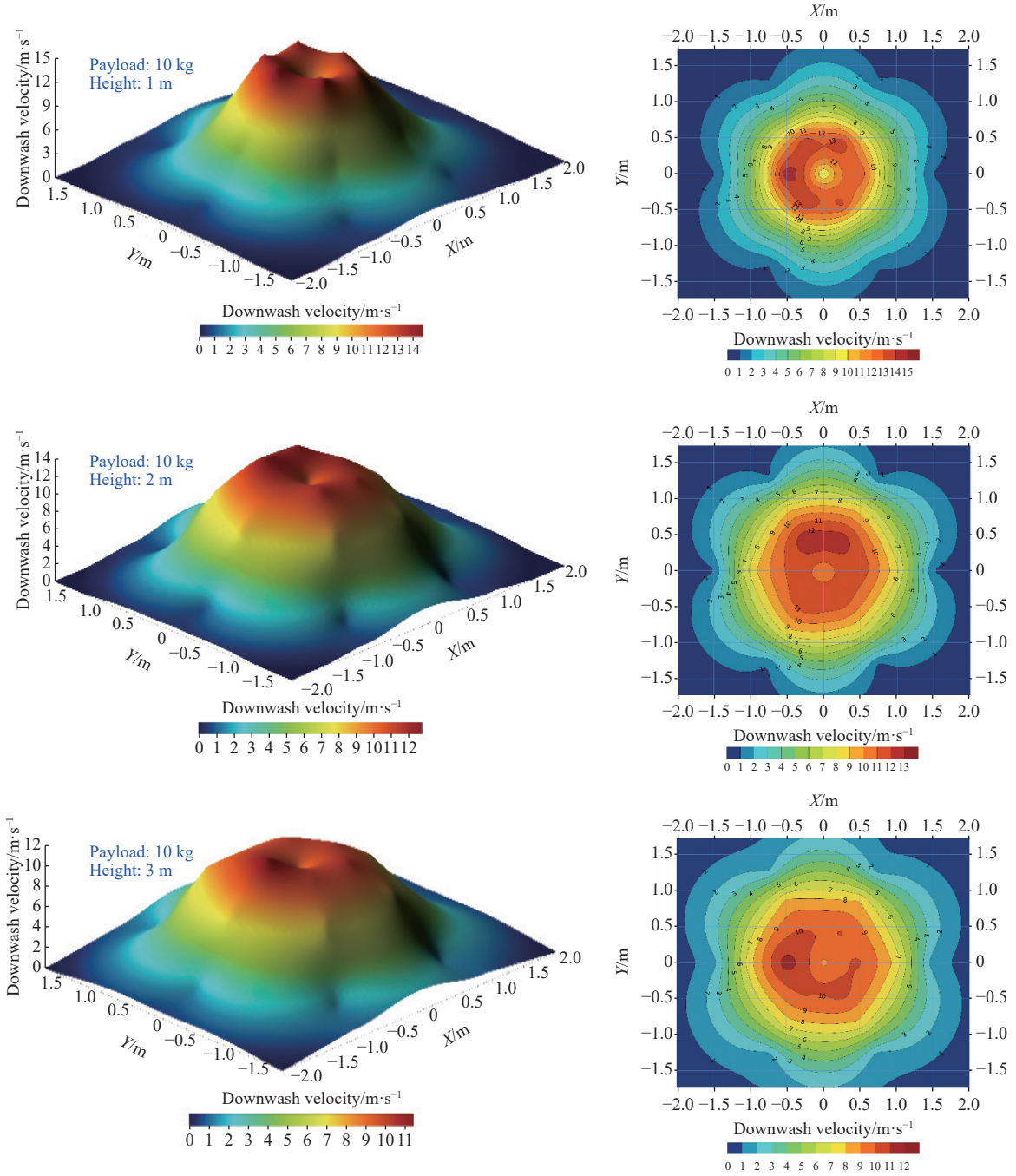


Figure 15 Downwash airflow distribution velocity at 10 kg payload (1.0 m, 2.0 m and 3.0 m)

**Table 7 Sprayer droplet characteristics of UAV sprayer and knapsack manual at each position and locations in rice crop**

| Method of spray | Position of WSP on leaf | Location of WSP in field | Spray droplet size/$\mu$m | Droplet density/ Droplets·cm$^{-2}$ | Coverage/ % | Deposition rate/$\mu$L·cm$^{-2}$ |
|---|---|---|---|---|---|---|
| UAV sprayer | Upper | U1 | 576±15.18 | 36±2.52 | 8.66±0.82 | 0.88±0.09 |
| | | U2 | 578±9.61 | 33±3.61 | 8.23±1.03 | 0.82±0.11 |
| | | U3 | 546±14.01 | 39±5.69 | 9.60±0.65 | 0.97±0.12 |
| | Bottom | B1 | 555±19.86 | 30±2.31 | 8.25±0.67 | 0.76±0.14 |
| | | B2 | 549±17.00 | 29±4.04 | 8.31±0.66 | 0.85±0.10 |
| | | B3 | 465±10.58 | 31±2.08 | 8.52±1.11 | 0.80±0.13 |
| Knapsack sprayer | Upper | U1 | 621±6.56 | 44±3.61 | 9.74±0.87 | 1.20±0.08 |
| | | U2 | 658±16.82 | 37±2.52 | 11.12±1.47 | 1.24±0.10 |
| | | U3 | 678±9.29 | 41±7.94 | 10.02±0.22 | 1.47±0.06 |
| | Bottom | B1 | 524±7.21 | 14±3.61 | 2.66±0.39 | 0.26±0.04 |
| | | B2 | 447±7.55 | 16±3.51 | 3.21±0.83 | 0.34±0.05 |
| | | B3 | 463±6.08 | 10±2.08 | 2.71±0.58 | 0.27±0.05 |

distribution model along the radial direction of the rotor with different hover height and payload and also clearly understanding the changing law of the airflow under the rotor.

## [References]

[1] Xue X Y. Applications of modern pesticide aerial application technology and the impact on rice quality. PhD dissertation. Jiangsu: Nanjing Agricultural University, 2013: 172p.

[2] Wang X N, He X K, Song J L, Wang Z C, Wang C L, Wang S L, et al. Drift potential of UAV with adjuvants in aerial applications. Int J Agric & Biol Eng, 2018; 11(5): 54–58.

[3] Bae Y, Koo Y M. Flight attitudes and spray patterns of a roll-balanced agricultural unmanned helicopter. Appl. Eng. Agric., 2013; 29: 675–682.

[4] Yang S. Spray droplet deposition and distribution inside crop canopy and control efficiency applied by unmanned aerial vehicle. Master dissertation. Beijing: Chinese Academy of Agricultural Sciences, 2014: pp.1–44.

[5] Li J Y, Lan Y B, Shi Y Y. Research progress on airflow characteristics and field pesticide application system of rotary-wing UAV. Transactions of the

CSAE, 2018; 34(12): 104–118. (in Chinese)
[6] Lan Y B, Qian S C, Chen S D, Zhao Y J, Deng X L, Wang G B, et al. Influence of the downwash wind field of plant protection UAV on droplet deposition distribution characteristics at different flight heights. Agronomy, 2021; 11(12): 2399.
[7] Luo B T. Research on droplet deposition characteristics of large-scale plant protection UAV spraying operation. Master dissertation. Jiangsu: Jiangsu University, 2018; 56p.
[8] Li J Y, Zhou Z Y, Lan Y B, Hu L, Zang Y, Liu A M, Luo X W, Zhang T M. Distribution of canopy wind field produced by rotor unmanned aerial vehicle pollination operation. Transactions of the CSAE, 2015; 31(3): 77–86. doi: 10.3969/j.issn.1002-6819.2015. 03.011.
[9] Wu Y L, Qi L J, Zhang H, Musiu E M, Yang Z P, Wang P. Design of UAV downwash airflow field detection system based on strain effect principle. Sensor, 2019; 19(11): 2630.
[10] Yang F B, Xue X Y, Zhang L, Sun Z. Numerical simulation and experimental verification on downwash air flow of six-rotor agricultural unmanned aerial vehicle in hover. Int J Agric & Biol Eng, 2017; 10(4); 41–53.
[11] Guo Q, Zhu Y, Tang Y, Hou C, He Y, Zhuang J, et al. CFD simulation and experimental verification of the spatial and temporal distributions of the downwash airflow of a quad-rotor agricultural UAV in hover. Computers and Electronics in Agriculture, 2020; 172: 105343.
[12] Zhang H X. Investigations on fidelity of high order accurate numerical simulation for computational fluid dynamics. ACTA Aero Dynamica Sinica, 2016; 34(1): 1–4.
[13] Yang F B, Xue X Y, Cai C, Sun Z, Zhou Q Q. Numerical simulation and analysis on spray drift movement of multirotor plant protection unmanned aerial vehicle. Energies, 2018; 11(9): 1–20.
[14] Bai X S, Dafsari R A, Lee J. Downwash flow measurement of the rotor blade for an agricultural spraying drone. KSME Conference paper, 2019, JEJU Island.
[15] Dixon David, Boon S, Silins U. Watershed‐scale controls on snow accumulation in a small montane watershed, southwestern Alberta, Canada. Hydrological Processes, 2014; 28(3): 1294–1306.
[16] Wang X N, He X K, Song J L, Wang Z C, Wang C L, Wang S L, Wu R C, Meng Y H. Drift potential of UAV with adjuvants in aerial applications. Int J Agric & Biol Eng, 2018; 11(5): 54–58.
[17] Tang Q, Zhang R R, Chen L P, Xu M, Yi T C, Zhang B. Droplets movement and deposition of an eight-rotor agricultural UAV in downwash flow field. Int J Agric & Biol Eng, 2017; 10(3): 47–56.
[18] Liu Q, Chen S D, Wang G B, Lan Y B. Drift evaluation of a quadrotor unmanned aerial vehicle (UAV) sprayer: Effect of liquid pressure and wind speed on drift potential based on wind tunnel test. Applied Sciences, 2021; 11(16): 7258.
[19] Wang L, Hou Q H, Wang J P, Wang Z W, Wang S M. Influence of inner tilt angle on downwash airflow field of multi-rotor UAV based on wireless wind speed acquisition system. Int J Agric & Biol Eng, 2021; 14(6): 19–26.
[20] Yang Z L, Ge L Z, Qi L J, Cheng Y F, Wu Y L. Influence of UAV rotor down-wash airflow on spray width. Transactions of the CSAM, 2018; 49(1): 116–122. (in Chinese)
[21] Zhang H Y, Lan Y B, Shen N W, Wu J Y, Wang T, Han J, et al. Numerical analysis of downwash flow field from quad-rotor unmanned aerial vehicles. International Journal of Precision Agricultural Aviation, 2020; 3(4): 1–7.
[22] Berner B, Chojnacki J. Use of drones in crop protection. IX International Scientific Symposium "Farm Machinery and Processes Management in Sustainable Agriculture", 2017. doi: 10.24326/fmpmsa.2017.9.
[23] Choi D S, Ma K C, Kim H J, Lee J H, Oh S A, Kim S G. Control standards of three major insect pests of Chinese cabbage (Brassica campestris) using drones for pesticide application. Korean Journal of Applied Entomology, 2018; 57(4): 347–354.
[24] Zhang H Y, Wen S, Chen C L, Liu Q, Xu T Y, Chen S D, et al. Downwash airflow field distribution characteristics and their effect on the spray field distribution of the DJI T30 six-rotor plant protection UAV. Int J Agric & Biol Eng, 2023; 16(2): 10–22.
[25] Wang C, He X, Wang X, Wang Z, Wang S, Li L, et al. Distribution characteristics of pesticide application droplets deposition of unmanned aerial vehicle based on testing method of deposition quality balance. Transactions of the CSAE, 2016; 32(24): 89–97.
[26] Liu X, Zhang W, Fu H B, Fu X M, Qi L Q. Distribution regularity of downwash airflow under rotors of agricultural UAV for plant protection. Int J Agric & Biol Eng, 2021; 14(3): 46–57.
[27] Tang Q, Zhang R R, Chen L P, Xu M, Yi T C, Zhang B. Droplets movement and deposition of an eight-rotor agricultural UAV in downwash flow field. Int J Agric & Biol Eng, 2017; 10(3): 47–56.
[28] Tan F, Lian Q, Liu C L, Jin B K. Measurement of downwash velocity generated by rotors of agriculture drones. Imateh-Agricultural Engineering, 2019; 55(2): 141–150.
[29] Xue X Y, Tu K, Qin W C, Lan Y B, Zhang H H. Drift and deposition of ultra-low altitude and low volume application in paddy field. Int J Agric & Biol Eng, 2014; 7(4): 23–28.
[30] Ahmad F, Zhang S, Qiu B, Ma J, Xin H, Qiu W, et al. Comparison of water sensitive paper and glass strip sampling approaches to access spray deposit by UAV sprayers. Agronomy, 2022; 12(6): 1302.
[31] Guo S, Li J Y, Yao W X, Zhan Y L, Shi Y Y. Distribution characteristics on droplet deposition of wind field vortex formed by multi-rotor UAV. PloS one, 2019; 14(7): e0220024.
[32] Martin D, Singh V, Latheef M A, Bagavathiannan M. Spray deposition on weeds (*Palmer amaranth and Morningglory*) from a remotely piloted aerial application system and backpack sprayer. Drones, 2020; 4(3): 59.
[33] Zhu H, Salyani M, Fox R D. A portable scanning system for evaluation of spray deposit distribution. Computers and Electronics in Agriculture, 2011; 76(1): 38–43.
[34] Modather M, Yahya A, Adam M, Suhaizi A, Elsoragaby S. Evaluation of pesticide spraying quality in wetland rice cultivation in Malaysia. Konvensyen Kebangsaan Kejuruteraan Pertanian Dan Makanan 2019, Putrajaya, Malaysia, 2019; pp.233–237.
[35] Chen S D, Lan Y B, Zhou Z Y, Ouyang F, Wang G B, Huang X, et al. Effect of droplet size parameters on droplet deposition and drift of aerial spraying by using plant protection UAV. Agronomy, 2020; 10(2): 195.